Physics – Uspekhi **38** (6) 609 – 623 (1995)

PACS numbers: 14.20.–c; 14.40.–n; 13.75.–n

Fractal analysis and Feigenbaum universality in hadron physics

A V Batunin

Contents

Abstract. The current state of the mathematical formalism commonly used in the study of fractals — infinite sets with noninteger Hausdorff dimension — is briefly revealed. The application of fractal analysis to hadron physics is shown. In this connection, the hypothesis on the presence of the Feigenbaum universality in hadron multiproduction characteristics is discussed.

1. Introduction

Fractal sets (fractals) are infinite sets with noninteger Hausdorff dimension [1]. In practice, however, we always deal with finite sets: a set of charged particles generated by hadron collision; ice crystals combining together to form a pattern on a glass window; eddies in turbulent flow; etc. Nevertheless, it turns out that at a sufficiently large ratio (of the order of a hundred or more) of the size of a whole object to the typical size of its constituents, the finiteness of the number of these constituents can be ignored on scales much greater than their size, so that one may apply the mathematical formalism developed for proper fractals.

This has been done during the past twenty years in almost all fields of physics: from the physics of the solid state (investigations of spin glasses) and fluids (analysis of appearance of turbulence) to astrophysics (the study of stellar, galactic, and cosmic dust cloud distributions) which allows one to reveal very interesting features eluding earlier researchers. (For one of the latest cross-disciplinary collected papers see Ref. [2].) In hadron physics, the ideas of fractality took hold only fifteen years ago [3 – 5], but serious interest was displayed somewhat later, after the practically simultaneous publication of two articles: by Bialas and Peschanski [6] and by Dremin [7]. The former authors proposed to study intermittency in charged particle distributions in the momentum space by means of factorial moments, while Dremin was the first to determine the dimension of the intrinsic motion of partons in hadrons.

Over the years fractal analysis has became recognised as one of the most powerful tools for the study of the dynamics of multihadron generation. In my opinion, it is imperative to collect and order the material concerning the theory of fractals and its applications in hadron physics, strewn over a lot of fine books, reviews [8 – 12], and original papers, making it brief and understandable for those who wish to study the subject.

This review consists of two parts. In the first one, I introduce the notions which are necessary for the discription of infinite sets: cardinality, topological invariants (Lebesque and inductive dimensions); Hausdorff dimension, generalised Renyi dimensions, and the spectral function depending on the space metric. Also the main notions of stochastic analysis proposed recently by Schertzer and Lovejoy [13] are given: 'calm' and 'wild' singularities, codimensions, the trace moment. In this part, I have tried to avoid, where possible, too rigorous mathematical proofs and mathematical terms not commonly used in the physical literature. The interested reader can easily find them in the relevant references.

In the second part, I show how fractal analysis is applied in practice. As an example, one of the well-known attractors — the Feigenbaum attractor — is considered as well as its finite approximations, the limit 2^m-cycles. The latter characterise the transition from order to chaos for a lot of nonlinear dynamical systems. Next I describe the Feigenbaum – Jensen – Procaccia method that enables one

A V Batunin Theory Division, Institute for High Energy Physics, Protvino, 142284 Moscow Province
E-mail: batunin@mx.ihep.su

Received 24 January 1995
Uspekhi Fizicheskikh Nauk **165** (6) 645 – 660 (1995)
Translated by the author and A Tybulewicz; edited by J R Briggs

to extract dynamical information from fractal structure data (a transfer matrix method) which is then applied in hadron physics. The results obtained suggest that the dynamics responsible for the observed charged particle distributions may be that of infinitely doubling bifurcations giving rise to the Feigenbaum attractor at asymptotically high energies.

It should be noted, however, that just accepting this hypothesis does not allow one unambiguously to write down the equations governing the dynamics of the process under consideration, since too many nonlinear differential equations have solutions obeying the Feigenbaum universality. The situation looks paradoxical — we can predict the behaviour of solutions to the equation which we do not know! Moreover, still for some known equation it is impossible to elucidate a priori (i.e. before solving) whether or not its solutions undergo period doubling as the governing parameter is varied. Thus, the problem of the nature of fractals in hadron physics remains to be solved. What actually may give rise to fractals is, for example, the equations of quantum chromodynamics [14] or the second-order phase transition [15, 16].

2. Mathematical formalism

2.1 Cardinality of sets

By a set is meant hereafter a set with an infinite number of elements (infinite set), unless otherwise specified. To compare one infinite set with another, in 1874 George Cantor [17, 18] introduced the notion of cardinality, or the cardinal number of a set. Under this definition, two sets have the same *cardinality* (i.e. they are equivalent) if a one-to-one correspondence (which does not need to be continuous) exists between their elements. Set A has a larger cardinality then set B if for any map of one set onto another an excess of elements of the set A remains.

The cardinality of an empty set is taken to be equal to zero. The next set in order of cardinality is that of all the natural numbers, which is called the *counting* set. Any finite set is obviously equivalent in cardinality to a part of the series of natural numbers and is called *no larger than counting*. The set of rational numbers and the set of algebraic numbers are counting sets. An association of counting number of counting sets is also a counting set. The set of irrational numbers and the set of real numbers come next in order of cardinality, the cardinality of the *continuum*. The set of all internal points of the unit interval [0, 1] has the cardinality of a continuum as well. {The points inside [0, 1] can be matched one-to-one with the points in entire real line through, say, the function $y = (1/\pi)\,\mathrm{arccot}\,x$.}

The cardinality of all the points in a plane (a two-dimensional continuum) is equal to the cardinality of the set of real numbers, i.e. the cardinality of a continuum. Moreover, the same cardinality characterises the continuum of an infinite but countable number of dimensions and the set of all *continuous* real functions of a real variable. Otherwise, the set of *all* real functions (including *discontinuous* ones) of a real variable has cardinality larger than the cardinality of a continuum.

Note that the equality between the cardinalities of any countable dimensional continuum — i.e. the existence of a one-to-one correspondence between their elements — is reached at the expense of a *discontinuity* in such a correspondence. The *continuity* and *one-to-one correspondence* of a map only in one direction also does not ensure that the continuum of different dimensions can be distinguishable. One such example is the Peano curve [19] that maps an interval onto a square continuously and in a one-to-one manner.

One may require *one-to-one correspondence* and *continuity* not only for a map but also for the relevant inverse map (a so-called *homeomorphism*). Then one can introduce a characteristic which is invariant under such homeomorphic maps — the *dimension* of the set.

2.2 Topological dimension

Quantities which are invariant under homeomorphic maps are called topological invariants. Two definitions of the dimension of a set A are recognised: the inductive dimension, $\mathrm{ind}\,A$, and the Lebesque dimension, $\dim A$.

H Poincare in 1912 sketched the first definition of the inductive dimension in his article "Why does space have three dimensions?" [20]: "To divide spaces it is necessary to use sets called surfaces; to divide surfaces it is necessary to use sets called lines; to divide lines it is necessary to use sets called points...". In modern usage the definition of the inductive dimension dating back to Brauer [21], Urison, and Menger [22, 23] is as follows: A set A has $A \leqslant n$, n integer, if for any neighbourhood Ox of a point $x \in A$ there exists a neighbourhood $O_1 x \in Ox$, whose boundary G has $\mathrm{ind}\,G \leqslant n-1$. Under this definition, an empty set has the dimension -1. A set is *zero-dimensional* if any of its points has arbitrarily small neighbourhoods with an empty boundary. For example, the following sets are zero-dimensional:

— any nonempty finite or counting set;
— the set of real rational numbers;
— the set of real irrational numbers;
— any set of real numbers that does not contain an interval;
— the set of points belonging to n-dimensional Euclidean space, with all coordinates of the points being rational numbers.

Note that all zero-dimensional sets are *nonconnected*, i.e. they can be divided into nonempty nonintersecting sets. However, the converse is not true: for any n there exists a completely nonconnected n-dimensional set [22, 23].

The Lebesque dimension [24] for set A, $\dim A$, is defined by means of the cover *multiplicity* (the highest integer number n for which there exist n sets with nonempty intersection in the given system of sets).

The dimension $\dim A$ of a set A is the least integer numbers n such that for any $\varepsilon > 0$ there exists a closed cover of multiplicity $\leqslant n+1$, with the diameter of each cover set being no greater than ε.

In particular, the Lebesque definition of dimension implies that any two-dimensional ($n = 2$) set can be covered by infinitesimal sets in such a way that each cover set borders no more than two other sets at any point on its boundary, ($n + 1 = 3$), and cannot be covered by infinitesimal sets if each cover set would border only one other set at every point of its boundary.

It was proved [22] that the inductive dimension and the Lebesque one for the same set A coincide:

$$\dim A = \mathrm{ind}\,A \ . \tag{1}$$

For any two sets A and B the following inequality is true [23]:

$$\dim(A \cup B) \leqslant \dim A + \dim B + 1 \ . \tag{2}$$

Any n-dimensional set can be represented as a sum of $n+1$ zero-dimensional sets and cannot be represented as a sum of a lesser number of zero-dimensional sets. The dimension of n-dimensional Euclidean space E_n equals n.

Any metric set A with countable basis, with $\dim A \leqslant n$, can be mapped homeomorphically onto a Euclidean space E, with $\dim E = 2n+1$ [25]. The number $2n+1$ cannot be reduced, i.e. there exist n-dimensional spaces that cannot be mapped homeomorphically onto E_{2n}. For example, a line (dim = 1) exists that cannot be mapped homeomorphically onto a plane (dim = 2) but can be onto a three-dimensional Euclidean space (dim = 3) [23].

The topological invariant, the dimension, turns out to be related to the metric notion, *the measure*, since an n-dimensional space has a positive n-dimensional measure (the converse in general is not true).

2.3 Measure and Hausdorff dimension

A d-dimensional measure for any real positive number $0 \leqslant d < \infty$ was introduced by Hausdorff [26] in 1919:

Let $A = A_1 \cup A_2 \cup \ldots$ be an arbirtrary partition of a set A into a counting number of subsets A_i with diameters $\delta(A_i) < \varepsilon$. Then for any $\varepsilon > 0$, we find

$$m_d^{\varepsilon} = \inf \sum_{i=1}^{\infty} \delta^d(A_i) \ . \tag{3}$$

Let us put

$$m_d(A) = \sup_{\varepsilon > 0} m_d^{\varepsilon}(A) \ , \tag{4}$$

then $m_d(A)$ is called the d-dimensional measure of the set A. Obviously, $m_0(A) = 0$ if A is an empty set; $m_0(A) = n$ if A is a finite set containing n points, and $m_0(A) = \infty$ if A is an infinite set.

The Hausdorff measure, $m_d(A)$, is a nonincreasing function of d for a given set A. Moreover, from the inequality $d < g$ and $m_d(A)$ it follows that $m_g(A) = 0$.

The *Hausdorff dimension*, D_{H}, of a set A is the upper bound (sup) of the set of all real numbers d such that $m_d(A) > 0$. Two important distinctions between D_{H} and the topological dimension $\dim A$ should be stressed:

— D_{H} is not necessarily an integer number;

— D_{H} is not a topological invariant, i.e. it depends on the metrics defined on a given set.

It is remarkable, however, that the lower bound (inf) of all D_{H}s corresponding to all possible metrics on a given set is its topological dimension [27]:

$$\inf D_{\mathrm{H}}(A) = \dim A \ . \tag{5}$$

It is commonly accepted to calculate D_{H} in the following way. Cover the given set A entirely by a system of closed sets A_i with diameters $\delta(A_i) < \varepsilon$. Find the minimal number $N(\varepsilon)$ of such sets for every ε. Clearly, $N(\varepsilon)$ is positive for any $\varepsilon > 0$ and grows infinitely as $\varepsilon \to 0$ only if A does not consist of a finite number of points. Let a positive number c exist such that the inequality

$$N(\varepsilon) \geqslant \frac{c}{\varepsilon^r} \quad \text{for any} \quad \varepsilon > 0 \ , \tag{6}$$

holds, where r is a real number. Then

$$D_{\mathrm{H}} = \lim_{\varepsilon \to 0} \inf \left[-\frac{\log N(\varepsilon)}{\log \varepsilon} \right] \ . \tag{7}$$

Find by this formula the Hausdorff dimension of some well-known fractal sets (we reach fractals proper at last!).

The *Cantor set* (CS) is defined as the set of real numbers that can be represented as the sum

$$\sum_{i=1}^{\infty} \frac{a_n}{3^n} \ , \quad a_n = 0 \quad \text{or} \quad 2 \ . \tag{8}$$

One can imagine CS, for simplicity, as the set of points remaining after the following (infinite) procedure: take the unit interval, divide it into three equal pieces and remove the middle piece; then again divide each of the remaining pieces (1/3 long) into three equal smaller pieces, etc. One can easily check that the sum of lengths, L, of the removed pieces is equal to one exactly:

$$L = \frac{1}{3} + \frac{2}{9} + \frac{4}{27} + \ldots = \frac{1}{3} \sum_{k=1}^{\infty} \left(\frac{2}{3} \right)^k = 1 \ .$$

(The same result can be obtained if at every step of the procedure one removes any finite part instead of one third of the piece.) This confirms that the linear measure of CS equals zero. Find its D_{H}. At the nth step of the construction procedure, 2^n intervals $(1/3)^n$ long each are needed to cover CS. Therefore,

$$D_{\mathrm{H}}^{\mathrm{KM}} = \lim_{n \to \infty} \left(-\frac{\log 2^n}{\log (1/3)^n} \right) = \frac{\log 2}{\log 3} = 0.630929 \ldots \tag{9}$$

By analogy with CS, one can find for the *Koch curve* — the curve of infinite length surrounding a finite area of a plane [28] — $D_{\mathrm{H}} = \log 4 / \log 3 = 1.261850 \ldots$. The *Serpinski carpet* — an analogue of CS on the square — has $D_{\mathrm{H}} = \log 8 / \log 3 = 1.892789 \ldots$, the *universal Menger curve* — an analogue of CS on the cube — has $\log 20 / \log 3 = 2.727833 \ldots$ [23].

Note that the three latter fractals have a topological dimension (dim) of one, whereas dim CS is zero..

When we calculated the Hausdorff dimension for a given set the metric was assumed to be the same over the whole set. But what if different regions of the set have different metrics? In other words, when some regions are more 'dense' than others?

The following section answers this question.

2.4 Renyi dimensions

Cover again a given set A with a finite system of closed subsets A_i with the diameters $\delta_i < \varepsilon$ ($\varepsilon > 0$), and define the minimal number $N(\varepsilon)$ of such subsets for every ε. On every subset A_i let its own metric act so that the corresponding Hausdorff dimension is equal to $D_{\mathrm{H}}(A_i)$. To each subset A_i the relevant weight p_i is ascribed, defined as the probability for an element of the set A to belong simultaneously to the subset A_i. In the case of the approximation of infinite sets A and A_i by finite ones that contain N and N_i elements, respectively, one can find p_i in the following way:

$$p_i = \lim_{N \to \infty} \frac{N_i}{N} \ .$$

In practice, when one investigates fractal phase trajectories one usually takes as p_i the quantity inversely proportional

to the time between two successive visits of the given set A_i by a point on the phase space trajectory. Clearly, the more dense A_i is (the more its elements are contained in a given volume of the phase space) the larger its weight is. It should be emphasised that, according to such a definition, the set with least Hausdorff dimension has the largest density because its elements are concentrated in minimal volumes of the phase space.

It is convenient to introduce the so-called singularity exponent, α_i, for a given weight p_i,

$$p_i(l) \propto l^{\alpha_i} , \tag{11}$$

which shows how rapidly the number of A_i elements inside some region of diameter l decreases as l is decreased. The smaller A_i is, the slower that decrease is, the more dense set we have.

For example, a monofractal at fixed l can be covered by N pieces, where $N \propto l^{-D_H}$, see Eqn (7). Consequently, for every such cover piece we get the same $p_i = 1/N$. Then

$$p_i(l) \propto l^{D_H} , \quad \text{i.e.} \quad \alpha_i = D_H . \tag{12}$$

In the case of a multifractal (i.e. a fractal set consisting of monofractals with different Hausdorff dimensions), we obtain a spectrum of singularities, $\alpha_{min} < \alpha_i < \alpha_{max}$.

By analogy with thermodynamics, one can define a function $\Gamma(q, \tau)$, which is called the partition function. Obviously, it generalises the Hausdorff measure [Eqn (3)] to multifractals. Each subset enters $\Gamma(q\ \tau)$ with its own weight p_i:

$$\Gamma(q,\tau) = \lim_{\varepsilon \to 0} \sum_{i=1}^{N(\varepsilon)} p_i^q \delta_i^{-\tau} . \tag{13}$$

At $q = 0$, the function $\Gamma(q, \tau)$ reduces to the usual $(-\tau)$-dimensional Hausdorff measure $m_{-\tau}(A)$ for the whole set, see Eqns (3) and (4), so that the corresponding value $-\tau(q = 0)$ is equal to the Hausdorff dimension of the set A,

$$-\tau(0) = D_H(A) . \tag{14}$$

One can show [9, 29] that for every value of q there is also a unique value of $\tau(q)$, such that the function $\Gamma[q, \tau(q)]$ has a positive-definite value $0 < \Gamma[q, \tau(q)] < \infty$. Then, for any real value of q one can introduce *generalised Renyi dimensions* D_q,

$$\tau(q) = D_q(q-1) . \tag{15}$$

By such a definition, the Renyi dimension D_0 is equal to the Hausdorff dimension D_H of the set A. Usually, an additional normalisation condition is imposed, $\Gamma(q, \tau) = 0$ for all q and $\tau(q)$, for which $\Gamma(q, \tau)$ is positive and finite. In order that the normalisation condition for $\Gamma(q, \tau)$ turn into the normalisation condition for the weighted sum of subsets of set A,

$$\sum_{i=1}^{\infty} p_i = 1 , \tag{16}$$

the equality $\tau(1) = 0$ must be obeyed. From Eqn (13) it follows that at $q \gg 0$, subsets with the largest weight give the main contribution to $\Gamma(q, \tau)$, i.e. the densest subset with minimal α. Substituting Eqns (11) and (15) into Eqn (13) and requiring $\Gamma(q, \tau) = 1$ we obtain $D_\infty = \alpha_{min}$. Analogously, at $q \ll 0$, subsets with smallest weight (i.e. most rarefied subsets with maximal α) will give the main contribution to α, and $D_{-\infty} = \alpha_{max}$. Therefore, D_∞ is equal to the Hausdorff dimension of the most dense subsets of the set A, whereas $D_{-\infty}$ is equal to the Hausdorff dimension of the most rarefied subsets.

The next step is to define how many subsets with the given singularity α_i are inside the set A. In other words, one needs to determine the dimension $f(\alpha_i)$ of the fractals with the singularity α_i inside the multifractal A. In accordance with Eqn (7) for the Hausdorff dimension, we can write for the number of pieces of the diameter l covering the fractals with the singularity α_i,

$$n(a_i, l) \propto l^{-f(\alpha_i)} . \tag{17}$$

If α is continuous with the density $\rho(\alpha)$ then the number of fractals with dimensions in the interval $(\alpha, \alpha + d\alpha)$ will obey the following law:

$$n(\alpha, l) = d\alpha\, \rho(\alpha) l^{-f(\alpha)} . \tag{18}$$

Then, we substitute the expression for p_i from Eqn (12) into Eqn (13), pass to the limit $l \to 0$, replace the summation over i by integration over α, and finally obtain

$$\Gamma(q,\tau) = \lim_{l \to 0} \sum_{i=1}^{N(l)} l_i^{q\alpha - \tau(q)} = l^{-\tau(q)} \int d\alpha\, \rho(\alpha) l^{q\alpha - f(\alpha)} = 1 . \tag{19}$$

The integral can be calculated by the method of steepest descent since the region with the smallest exponent gives the greatest contribution as $l \to 0$. Obviously, this minimum is defined by two conditions:

$$\left[q\alpha - f(\alpha)\right]' = 0 , \quad \left[q\alpha - f(\alpha)\right]'' > 0 , \tag{20}$$

wherefrom we immediately get

$$f'(\alpha_0) = q , \quad f''(\alpha_0) < 0 . \tag{21}$$

Note that here α_0 is already a function of q. Then we replace the value of the integral in Eqn (19) by the value of the integral function at the extremum point, taking into account the normalisation condition for $\rho(\alpha)$, and obtain

$$\tau(q) = q\alpha_0(q) - f\left[\alpha_0(q)\right] . \tag{22}$$

The function $f(\alpha)$ is called the spectral function for a given multifractal, and Fig. 1 shows a typical example. It is easy to see that $f(\alpha)$ is related to the function $\tau(q)$ via the Legendre transform. Indeed, substituting the first expression from Eqn (21) into Eqn (22), we obtain

$$\tau(q) = \alpha f'(\alpha) - f(\alpha) . \tag{23}$$

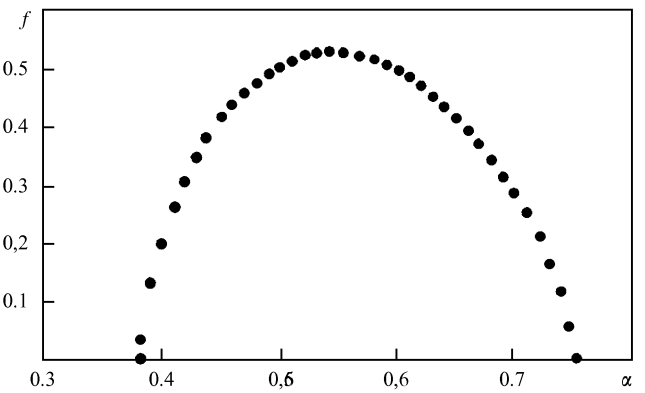

Figure 1. Spectral function of the Feigenbaum attractor, calculated on the basis of formula (55).

The converse formula is also true:

$$f(\alpha) = q\tau'(q) - \tau(q), \quad \text{since} \quad \alpha(q) = \tau'(q). \tag{24}$$

Certainly, in the case of a monofractal the spectral function 'shrinks' to a δ-function, since the whole monofractal is characterised by a single value of α that equals its Hausdorff dimension [see Eqn (12)], and $f(\alpha) = \alpha$.

A typical multifractal has a finite number both of the most concentrated subsets and of the most rarefied ones (most often only one); therefore, the set of such subsets is zero-dimensional (see Section 2.2) and the spectral function at these points comes to zero,

$$f(\alpha_{\min}) = f(\alpha_{\max}) = 0 . \tag{25}$$

From Eqn (21), we find that at the point $\alpha(0)$ the spectral function has a maximum. From Eqns (24) and (14), it follows that this maximum is equal to the Hausdorff dimension of the multifractal,

$$f_{\max}(\alpha) = f\big[\alpha(0)\big] = -\tau(0) = D_{\mathrm{H}}(A) . \tag{26}$$

As a rule, for a given multifractal, one calculates first the $\tau(q)$-dependence [or $q(\tau)$, if it is more convenient] and then finds its spectral function from Eqn (24).

2.5 Stochastic analysis

The theory given above can be called the 'geometrical' analysis of fractals. Unfortunately, this standard theoretical framework presupposes very restrictive calmness and regularity assumptions. This was noted in a recent work by Schertzer and Lovejoy [13], where they proposed a more general approach to the study of fractals, so-called 'stochastic' analysis. Later in this section I outline its basic statements, referring the interesting reader to the original papers [13, 30, 31].

Consider again a set A consisting of subsets A_i with the corresponding weights p_i and singularity exponents α_i, see Eqn (11). We will take the numbers p_i as corresponding to some (highly intermittent) 'field' ψ, produced by successive iterations of the procedure of random modulation of larger structures into smaller ones with a given probability distribution (for example, the well-known α-model [6]). This approach is applied, in particular, to the description of energy transfer from large vortices to small ones in a turbulent fluid where the density of the energy flux plays the role of the field ψ.

Certainly, in accordance with a rigorous mathematical definition we get a field (infinite number of the degrees of freedom) only by an infinitely small scale of partition (or covering) of the given set A. At finite scales ($\sim l$), we obtain a descrete analogue of the field ψ_l, defined on the N_l sets with the weights p_i. Its behaviour can be characterised either by its probability distribution

$$\Pr(\psi_l \geqslant l^{-\gamma}) \propto l^{c(\gamma)} \tag{27}$$

or by the corresponding law for the statistical order-q moments (by means of a Laplace transform):

$$\langle \psi_l^q \rangle \propto l^{-K(q)} \propto \int l^{-q\gamma + c(\gamma)}\, \mathrm{d}c(\gamma) . \tag{28}$$

The exponent $c(\gamma)$ in Eqn (27) is a codimension since the probability distribution determines the fraction of the probability space occupied by the singularities exceeding the order γ. At scale l, the probability can be estimated as the ratio of the number $N_l(\gamma)$ of corresponding sets to the total number of sets N_l:

$$\Pr(\psi_l \geqslant l^{-\gamma}) \propto \frac{N_l(\gamma)}{N_l} , \tag{29}$$

cf. Eqn (10). What is the relation between γ, $c(\gamma)$, and $f(\alpha)$ introduced in Section 2.4? This relation can be deduced but only for the values $c(\gamma) \leqslant D$, where D is the dimension (Euclidean) of the embedding space. Indeed, by Eqns (7) and (18) we obtain $N_l \propto l^{-D}$ and $N_l(\gamma) \propto l^{-f(\gamma)}$. Now consider D-dimensional integration of the field ψ_l:

$$\Pi_l(A) = \int \psi_l \, \mathrm{d}^D \boldsymbol{x} . \tag{30}$$

$\Pi_l(A)$ corresponds to the energy flux (in turbulence) or the weight p_i (in fractals). From Eqns (27) and (29), we immediately get

$$\Pr\big[\Pi_l(A_i) \geqslant l^{\alpha_i}\big] \propto l^{D - f(\alpha_i)} , \tag{31}$$

where the relation $\int \mathrm{d}^D \boldsymbol{x} \propto l^D$ is used. Consequently,

$$\alpha = D - \gamma, \quad f(\alpha) = D - c(\gamma) . \tag{32}$$

The restrictiveness of the 'geometrical' approach is thus easily seen: α and $f(\alpha)$, by definition, are positive so that in D-dimensional space one can see only a part of the field ψ_l singularities, $\psi_l \leqslant \gamma$, $c(\gamma) \leqslant D$, so-called 'calm' singularities. The singularities with $\gamma > D$ are called 'wild'. Increasing D, if it is possible, one extends the range of observed singularities. Note that the quantities γ and $c(\gamma)$ are intrinsic field characteristics independent of D, while α and $f(\alpha)$ diverge as $D \to \infty$.

Write down a generalisation of the partition function, the so-called 'trace moment' for the field ψ_l observed on the set A with the diameter-l covering:

$$\mathrm{Tr}_A\, \psi_l^q = \left\langle \sum_A \psi_l^q l^{Dq} \right\rangle \propto \left\langle \sum_i \Pi_l^q(A_i) \right\rangle , \tag{33}$$

where $\langle \ldots \rangle$ indicates averaging over all realisations of the field ψ at the given scale l. The trace moment combines ensemble with spatial averaging. In particular, in hadron physics it corresponds to the averaging over all events at fixed bin size in momentum space. Remembering that $\Pi_l(A_i)$ corresponds to p_i on a fractal with an l-diameter covering, and using Eqn (13), we obtain from Eqns (33) and (28):

$$\mathrm{Tr}_A\, \psi_l^q \propto l^{\tau(q)} \propto l^{D(q-1) - K(q)} , \tag{34}$$

relating $\tau(q)$ (depending on D) and $k(q)$, the intrinsic quantities of field. Like $f(\alpha)$ and $\tau(q)$, the quantities $c(\gamma)$ and $k(q)$ are related via the Legendre transform:

$$K(q) = \gamma c'(\gamma) - c(\gamma), \quad q = c'(\gamma) \tag{35}$$

$$c(\gamma) = qK'(q) - K(q), \quad \gamma = K'(q) . \tag{36}$$

To summarise, we have seen that a geometrical approach to the study of fractals is limited. The values of the quantities α and $f(\alpha)$ depend on the dimension of the observing space and, thus, cannot play the role of intrinsic quantities of the fractal. In other words, the entire spectrum of singularities is inaccessible: first, because of the finiteness of D; second, because of the exceptional rarity of strong singularities (fluctuations) so that they are rather unlikely in a single realisation (separate event).

Thus, to get more complete information about the singularities of the field ψ (having the set A as its D-dimensional projection) one needs to increase D and the number of realisations (events) and then to average over them.

In particular, in hadron physics one proceeds from the projection on the rapidity axis ($D = 1$) to three-dimensional momentum space ($D = 3$) and gains a large number of events (of the order of a hundred thousand) in particle collisions.

Unfortunately, this is not sufficient since there exist stochastic processes generating fields with so-called 'hard' singularities. They are not localised in space: in the neighbourhood of some point $\boldsymbol{x}$, the limit $\lim_{l\to 0}\gamma_l(\boldsymbol{x})$ does not exist. Thus, they are in principle out of the scope of the geometrical version of fractal analysis. But this is the subject of a separate article, so I refer the interested readers to Refs. [13, 14, 30, 31]. In the second part of this review (Section 3.3), it will be shown nevertheless that a substantial amount of information about the process generating a given multifractal can be extracted in the framework of the geometrical approach.

3. Physics applications

In this chapter, it will be shown how the geometrical version of fractal analysis is applied in practice. More precisely, only the connection between this method and the Feigenbaum universality will be considered because other applications were described, for example, in Refs [9–12]. To begin with, we shall study abstract mathematical objects, the Feigenbaum attractor and its finite approximations — limit cycles; then we proceed to the study of real sets, charged particle distributions along the rapidity axis.

3.1 Obtaining $\tau(q)$-dependence

In practice, we always deal with finite sets, whether it is a set of points on the phase space trajectory or a set of charged particles generated in proton collision.

Divide a given set containing n_{tot} elements into N nonintersecting groups A_i, $i = 1, 2, \ldots, N$, with the same number of elements n. Obviously, $nN = n_{\text{tot}}$. Each group A receives the same weight $p_i = 1/N$ but different diameter (bin) δ_i. Consider, for example, a set of charged particles in the projection on the rapidity axis in a separate event so that y_i is the rapidity of the ith particle. Then the diameter δ_j may be found from the formula

$$\delta_j = |x_{jn} - x_{(j-1)n+1}| \,. \tag{37}$$

Here the subscript j labels the groups of particles ($j = 1, 2, \ldots, N$) while x_i is the coordinate of the ith particle on the unit interval [0, 1], obtained from the entire rapidity interval $[-y_{\max}, y_{\min}]$ by means of some smooth transformation, for example, $x_i = \frac{1}{2}(\tanh y_i + 1)$. Then, from Eqn (13) and the condition $\Gamma(q, \tau) = 1$, we get

$$\sum_{i=1}^{N} p_i^q \delta_i^{-\tau} = N^{-q} \sum_{i=1}^{N} \delta_i^{-\tau} = 1 \,. \tag{38}$$

From this, we immediately obtain

$$q(\tau) = \frac{1}{\log N} \sum_{i=1}^{N} \delta_i^{-\tau} \,, \tag{39}$$

and then the $\tau(q)$-dependence by inversion. This method — the same-weight method (SWM) — is applied in hadron physics only in the case when the velocities of all particles in a given event are known to a sufficiently high accuracy.

However, it is possible to find the $\tau(q)$-dependence directly. To to this, divide the entire rapidity interval into the same diameter-δ bins. Then the same diameter bins will correspond to different weights, $p_i = n_i/n_{\text{tot}}$, where n_i is the number of particles in the ith bin. More precisely, define the moments G_q [32],

$$G_q(\delta) = \sum_{i=1}^{N} p_i^q \,, \tag{40}$$

where the sum runs over all nonempty bins. Again, map the entire rapidity interval onto the unit interval [0, 1] by means of some smooth transformation. Then, for not too small a value of δ (i.e. if the number of empty bins is not too large), from the condition $\Gamma(q, \tau)$ it follows that

$$G_q(\delta) = \delta^{\tau(q)} \,, \qquad \tau(q) = \frac{\log G_q(\delta)}{\log \delta} \,. \tag{41}$$

In practice, this method turns out to be less exact than SWM. As an illustration, apply SWM to the Cantor set. On the nth step of its construction we have

$$p_i = \left(\frac{1}{2}\right)^n \,, \qquad \delta_i = \left(\frac{1}{3}\right)^n \,, \tag{42}$$

so that we immediately get from Eqn (13) and condition $\Gamma(q, \tau)$

$$\tau(q) = (q-1)\,\frac{\log 2}{\log 3} \,, \qquad \text{i.e.} \qquad D_q = \frac{\log 2}{\log 3} \tag{43}$$

for all q. From Eqn (24) it follows that

$$\alpha = D_q = \frac{\log 2}{\log 3} = \text{const} \,, \qquad f(\alpha) = D_q = \alpha = \text{const} \,, \tag{44}$$

as would be expected for a monofractal.

Below we apply the formalism considered to probably one of the best known multifractals — the Feigenbaum attractor. Moreover, in recent years a hypothesis was put forward on its presence in the characterictics of particle multiproduction in high-energy collisions [33–36].

3.2 Limit cycles and the Feigenbaum attractor

The Feigenbaum attractor is a multifractal on the interval [0, 1] gomeomorphic to the Cantor set. The Feigenbaum attractor can be obtained as a result of infinite series of period doubling bifurcations of limit cycles for one-dimensional one-parameter maps of the interval [0, 1]. (Recall that the bifurcation is called a qualitative sudden change in the behaviour of a solution to some nonlinear equation as the governing parameter is smoothly varied.) In order that such bifurcations are possible, the given maps must obey the following conditions [37]:

— have a unique maximum in the interval [0, 1];
— increase monotonically from the left of the maximum and decrease monotonically on the right of it;
— depend smoothly on the governing parameter;
— the Schwartzian of the map must be negative at the point of bifurcation.

Recall that the Schwartzian (the Schwartz derivative) of a function $f(x)$ is an expression of the form

$$\frac{f'''(x)}{f'(x)} - \frac{3}{2}\left[\frac{f''(x)}{f'(x)}\right]^2 .$$

Obviously, smooth maps with a quadratic maximum obey the conditions listed above; therefore, the Feigenbaum attractor can be obtained by iteration of the centre of the unit interval by means of, for example, a logistic map

$$x_{n+1} = \lambda x_n(1 - x_n) \tag{45}$$

at $\lambda = \lambda_\infty = 3.5699456\ldots$. If the governing parameter λ takes values on the interval $3 < \lambda < \lambda_\infty$ then the succession of the points x_n at $n \to \infty$ converges towards some limit 2^m-cycle ($m = 1, 2, \ldots$), corresponding to a given $\lambda = \lambda m$. Every such limit cycle can be considered as a finite approximation of the Feigenbaum attractor. When λ is smoothly increased within the interval $3 < \lambda < \lambda_\infty$ the periods of the limit cycles successively double, $2^m \to 2^{m+1}$, i.e. period-doubling bifurcations occur. The name 'attractor' in this case reflects the fact that all points from the interval [0, 1] except a counting set are attracted by means of Eqn (45) at $\lambda = \lambda_\infty$ to the Feigenbaum attractor [37, 38].

This multifractal received its name in 1978 in honour of its discover and investigator, the American scientist M Feigenbaum of Los Alamos. (For the Russian translation of his article see Ref. [39].) The main point of the discovery is that the cycle bifurcations for all maps obeying conditions listed above are described by two universal constants (the so-called Feigenbaum constants) [40, 41]:

$$\alpha_F = 2.5029078\ldots, \qquad \delta_F = 4.6692016\ldots . \tag{46}$$

The constant δ_F characterises the rate of convergence of the governing parameter critical values towards its limit value:

$$\lim_{m\to\infty} \frac{\lambda_m - \lambda_{m-1}}{\lambda_{m+1} - \lambda_m} = \delta_F , \tag{47}$$

while the constant α_F characterises the scale of successive 'splittings' of the limit cycle elements after each bifurcation:

$$\lim_{m\to\infty} \frac{|x_m - 1/2|}{|x_{m+1} - 1/2|} = \alpha_F , \tag{48}$$

where α_F denotes the limit 2^m-cycle element nearest to the cycle element $x = 1/2$.

One-dimensional one-parameter maps are commonly used in the study of the phase space trajectories of nonlinear dynamical systems, where they appear as Poincare maps [42]. (Recall that the Poincare map is a dependence of the form $\boldsymbol{x}(n+1) = \boldsymbol{G}[\boldsymbol{x}(n), \lambda]$, obtained by intersection of a phase space trajectory in d-dimensional phase space and $(d-k)$-dimensional hyperplane,

$$\boldsymbol{x}(n) = \{x_1(n), x_2(n), \ldots, x_{d-k}(n)\} .$$

The number n labels the succession of the points of intersection along the trajectory.) It turns out that the restrictions imposed on the maps (see above) are rather weak, so that plenty of real physical systems satisfy these restrictions. As a consequence, the Feigenbaum discovery led to an explosion of experiments confirming the existence of the universal constants [43].

One finds by Eqn (45) the limit superstable 8-, 16-, 32-, 64- and 2048-cycles. The prefix 'super' means that the given cycles contain element where the first derivative of the map vanishes (in our case, this is $x = 1/2$). The 2048-cycle reproduces with high accuracy the characteristics of the Feigenbaum attractor, see Ref. [29]. To obtain the $q(\tau)$-dependence we apply SWM since the coordinates of the cycle elements are known within the interval [0, 1] and may be determined to arbitrary accuracy [38]. The nearest cycle elements are joined in pairs generating a division of the unit interval into N subintervals ($N = 2^{m-1}$ for 2^m-cycle) each with weight $p_i = 1/N$. Setting various τ we find according to Eqn (39) the $q(\tau)$ dependence for every cycle. The generalised Renyi dimensions, D_q, were then found by Eqn (15). In Table 1, the obtained values D_∞, D_0, and $D_{-\infty}$, are shown for the limit 2^m-cycles and the Feigenbaum attractor.

Table 1.

2^m	D_∞	D_0	$D_{-\infty}$
8	0.284	0.358	0.446
16	0.310	0.403	0.519
32	0.324	0.430	0.563
64	0.334	0.448	0.593
∞	0.377...	0.537...	0.755...

Recall that

$$D_\infty = D_H^{\min} , \qquad D_{-\infty} = D_H^{\max} \tag{49}$$

among all D_H for all subsets of the set A (see Section 2.4). For the Feigenbaum attractor, $D_H^{\min}$ is generated by subsets homeomorphic to the Cantor set with the rescaling parameter α_F^{-2}, whereas $D_H^{\max}$ is generated by subsets with the rescaling parameter α_F^{-1} [29]. In other words, to calculate the limit Renyi dimensions for the Feigenbaum attractor we use Eqn (42) where, instead of 1/3, we substitute first α_F^{-2} and then α_F^{-1}, and from Eqn (43) we obtain respectively

$$D_\infty^F = \frac{\log 2}{2\log\alpha_F} = 0.377756\ldots , \tag{50}$$

$$D_{-\infty}^F = 2D_\infty^F = \frac{\log 2}{\log\alpha_F} = 0.755512\ldots . \tag{52}$$

For Renyi dimensions with arbitrary q, the analytical dependence can be obtained by approximating the Feigenbaum attractor by a two-scale Cantor set [29], $\delta_1 = \alpha_F^{-1}$ and $\delta_2 = \alpha_F^{-2}$ with the same weights $p_1 = p_2 = 1/2$. Substituting these expressions into Eqn (13) we get for the 2^m-cycle in the limit case $m \to \infty$

$$\Gamma(q, \tau) = (p_1^q\delta_1^\tau + p_2^q\delta_2^\tau)^m = 1 . \tag{52}$$

Wherefrom

$$\alpha^\tau(\alpha^\tau + 1) = 2^q , \tag{53}$$

and

$$D_q^F = \frac{\tau(q)}{q-1} = \frac{\log(\sqrt{1/4 + 2^q} - 1/2)}{(q-1)\log\alpha_F} . \tag{54}$$

For the limit Renyi dimensions $D_{-\infty}^F$ and D_∞^F, Eqn (54) gives the exact values. For D_0^F, we obtain the value 0.525, which is only 2.5% different from the true value 0.537. For intermediate D_q^Fs, the accuracy is better than 2.5%.

From Eqn (54), it is easy to obtain an explicit expression for the spectral function of the Feigenbaum attractor $f_F(\alpha)$

$$f_F(\alpha) = \frac{\alpha\log\alpha - \alpha_1\log\alpha_1 - \alpha_2\log\alpha_2}{\log 2}\,,$$
$$\alpha_1 = 2\alpha - 2D_\infty\,, \qquad \alpha_2 = 2D_\infty - \alpha\,. \tag{55}$$

This is shown in Fig. 1.

3.3 Transfer matrix method

In this section, it will be shown how to use our knowledge of the fractal structure of the object under consideration (its Renyi dimensions) to obtain information about the dynamics that is responsible for generating of this object. This became possible owing to the transfer matrix method by Feigenbaum, Jensen, and Procaccia, 1986 [44]. The key idea of this method rests on an analogy between the process of refinement of the fractal measure and a transfer matrix theory of an appropriate Ising model [45].

Consider a finite cover of a given fractal by N non-intersecting pieces $\{\Delta_i\}$. Let as usual, δ_i be the diameter of the ith piece and p_i be its weight. Apply SWM (Section 3.1) to find the $q(\tau)$-dependence for the given set, i.e. consider such a covering of the fractal that all $p_i = 1/N$ are the same. Then, the function $q(\tau)$ can be found from Eqn (39). Increase successively the number of the pieces N according to power law, $N - N_n = a^n$, where n is a positive integer, $\alpha > 0$. Then for any n, we can label $\delta_i\,(1 \leqslant i \leqslant N)$ as $\delta_{\varepsilon_n,\ldots,\varepsilon_1}$, where ε_i takes on a values $0, 1, \ldots, a-1$ if a is an integer. If a is a fraction then ε_i takes on $[a]+1$ values $0, 1, \ldots, [a]$, where $[a]$ is the integer part of a. Hereafter we restrict ourselves to the case of integer as, for simplicity. Next define the daughter-to-mother ratio for the neighbouring 'generations' [44]:

$$\frac{\delta_{\varepsilon_{n+1},\varepsilon_n,\ldots,\varepsilon_1}}{\delta_{\varepsilon_n,\ldots,\varepsilon_1}} = \sigma_{\varepsilon_{n+1},\varepsilon_n,\ldots,\varepsilon_1}\,. \tag{56}$$

Suppose this ratio depends only on two latter indices ε_{n+1}, ε_n. Then $\sigma_{\varepsilon_{n+1},\varepsilon_n}$ defines a (transfer) matrix $a \times a$, so that any diameter can written as the product of the transfer matrix elements,

$$\delta_{\varepsilon_n,\ldots,\varepsilon_1} = \sigma_{\varepsilon_n\varepsilon_{n-1}}\sigma_{\varepsilon_{n-1}\varepsilon_{n-2}}\ldots\sigma_{\varepsilon_2\varepsilon_1}\delta_{\varepsilon_1}\,. \tag{57}$$

(with no summation). The summation appears when we substitute this expression into Eqn (39), where the sum on the right-hand-side becomes as follows:

$$\sum_{i=1}^{a^n}\delta_i^{-\tau} = \sum_{\forall\varepsilon}\left(\sigma_{\varepsilon_n\varepsilon_{n-1}}\sigma_{\varepsilon_{n-1}\varepsilon_{n-2}}\ldots\sigma_{\varepsilon_2\varepsilon_1}\delta_{\varepsilon_1}\right)^{-\tau}$$
$$= \sum_{\varepsilon_n,\varepsilon_1}\left[\sigma(\tau)\right]^n_{\varepsilon_n\varepsilon_1}\delta_{\varepsilon_1}^{-\tau} = \mathrm{Tr}\left[\sigma^n(\tau)\right] \tag{58}$$
$$\left[\sigma(\tau)\right]_{\varepsilon_j\varepsilon_k} \equiv \sigma^{-\tau}_{\varepsilon_j\varepsilon_k}\,.$$

We see that summation over the is transforms into summation over all possible ε, which, in turn, reduces to the production of the σ matrices. It should be clear by now how the analogy arises with the calculation of the partition function, Z_N, in a one-dimensional Ising model with nearest-neighbour interaction [45]:

$$Z_N = \sum_{\forall\varepsilon}\exp\left(-\frac{S}{kT}\right), \qquad S = E\sum_i\varepsilon_i\,\varepsilon_{i+1} + H\sum_i\varepsilon_i\,, \tag{59}$$

where ε_i is a spin variable at the ith site taking on m values, T is the temperature, E is the spin–spin coupling constant, and H is the applied magnetic field. In the simplest nontrivial case, $m = 2$, the corresponding transfer matrix $\sigma_{\varepsilon_i\varepsilon_j}$ appears as follows:

$$\sigma = \xi\begin{pmatrix}\exp(-J-K) & \exp J\\ \exp J & \exp(-J+K)\end{pmatrix},$$

where ξ is the normalisation factor, $J = E/kT$, $K = H/kT$. The number of spin states, m, at each site of the corresponding Ising chain determines the size of the transfer matrix. It shows how many times, a, the number of the fractal cover pieces increases at every step. The transfer matrix elements provide information on the scale of successive splittings of elements of a given fractal set at every step of its covering.

The size of the region of interaction depends on how far the 'memory' goes back in the definition of ratio (56). If we truncate the succession $\varepsilon_{n+1}, \varepsilon_n, \ldots, \varepsilon_1$ by ε_n then we get the nearest-neighbour interaction. Such a limitation is justified because we know that in many fractal sets, the 'memory' falls off exponentially.

Taking the trace in Eqn (58) reduces to the summation of nth powers of the eigenvalues λ_j for the matrix $\sigma(\tau)$:

$$\mathrm{Tr}\left[\sigma^n(\tau)\right] = \sum_{j=1}^{a}\lambda_j^n\,. \tag{60}$$

In the limit $n \to \infty$ (the so-called thermodynamic limit in the language of the Ising model), only the largest eigenvalue 'survives', λ_+, so that we obtain from Eqns (39), (58), and (60):

$$q_a(\tau) = \frac{\log\lambda_+(\tau)}{\log a}\,. \tag{61}$$

We use the subscript a to determine the function $q_a(\tau)$ from Eqn (39). Note that a and $\lambda_+(\tau)$ are related,

$$a^{q(\tau)} = \lambda_+(\tau)\,, \tag{62}$$

which follows immediately from Eqn (61).

Thus, for a given matrix $\lambda_+(\tau)$ we find the value a from the corresponding characteristic polynomial of the order $a \times a$. In lowest-order nontrivial case of 2×2 matrix (which corresponds to $1 \leqslant a \leqslant 2$) we get

$$\lambda_+^2(\tau) - \lambda_+(\tau)(\sigma_{00}^{-\tau} + \sigma_{11}^{-\tau}) + (\sigma_{00}\sigma_{11})^{-\tau} - (\sigma_{01}\sigma_{10})^{-\tau} = 0\,. \tag{63}$$

The matrix elements σ_{01} and σ_{10} appear only as a product, and thus $\lambda_+(\tau)$ depends on three scales. Hence, together with $\lambda_+(\tau)$ we have four unknown and, therefore, need at least four experimental points $\tau(q)$. As usual, one is taken at $q = 0$ since $\tau(0) = -D_0$ [see Eqn (14)].

Then, from Eqn 62 it follows that $\lambda(-D_0) = 1$, and we get from Eqn (63),

$$\sigma_{01}\sigma_{10} = \left[(1-\sigma_{00}^{D_0})(1-\sigma_{11}^{D_0})\right]^{1/D_0}\,. \tag{64}$$

Note that from Eqn (62) at $q = 1(\tau = 0)$ it follows that $a = \lambda_+(0)$. At $\tau = 0$, Eqn (63) gives two solutions for $\lambda_+(0)$ (and, thus, for a): $\lambda_+(0) = 2$ for any $\sigma_{ij} \neq 0$; and $\lambda_+(0) = (\sqrt{5}+1)/2$ at $\sigma_{00} = 0$ or $\sigma_{11} = 0$.

It is time to summarise. Suppose we know the $q(\tau)$-dependence for a given fractal and wish to know what dynamical process generates the given fractal (for example, a phase space trajectory or its Poincare section). By 'know

the dynamical process' I mean 'calculate the transfer matrix elements and the a value', since the latter unambiguously define the type of the corresponding Poincare section. 'Dynamics' means the dynamics relative to the corresponding governing parameter not the dynamics in time at the fixed value of the governing parameter. For example, the case $\alpha = 2$ corresponds to the period-doubling bifurcation dynamics.

A priori, the value a is unknown and, thus, the size of the transfer matrix is unknown too. Therefore, one begins as usual with the simplest nontrivial case of 2×2 matrices, solving the system of four linear equations (63). The a value is found then from Eqn (62). If the solutions exist and are sufficiently stable relative to various $q(\tau)$ then the study is finished here — the dynamics is taken to be found. If there are no solutions or they exist but change strongly at various $q(\tau)$ then one has to study the case of 3×3-matrices. If again there are no stable solutions one proceeds to the case of 4×4-matrices and so on.

It is necessary to make one remark. In experiments, only a finite precision, say, $\Delta\delta$ is accessible to measurement of the cover diameter of the fractal under consideration. The diameter fluctuations $\delta_i \to \delta_i + \Delta\delta$ cause the q-fluctuations, $q \to q + \Delta q$, where

$$\delta q \sim -\tau \Delta\delta \frac{N^{q(\tau+1)-q(\tau)}}{\log N} . \tag{65}$$

Therefore, to minimise the influence of experimental fluctuations on the finite result one needs to take τ-values near zero.

The transfer matrix method works if among the eigenvalues of σ matrix, there is one much larger than the others. Then the function $q_a(\tau)$ [Eqn (61)] fits with high accuracy the 'experimental' function $q(\tau)$ [Eqn (39)] on a sufficiently large interval.

One may apply the transfer matrix method to the limit cycles and Feigenbaum attractor in order to see that this method really allows one to reveal the period-doubling dynamics. Taking $q(\tau)$-dependence for each limit cycle and Feigenbaum attractor, we find according to Eqns (63) and (62) the elements of the corresponding transfer matrices and the a-value (see Table 2). The latter equals two with high accuracy for any limit cycle and Feigenbaum attractor as would be expected, while the values σ_{00}, σ_{11} and $\sigma_{01}\sigma_{10}$ converge from below to their limit values. These limit values by construction [see Eqn (56)], can be expressed via α_F:

$$\sigma_{00}^{AF} = \alpha_F^{-1} , \quad \sigma_{11}^{AF} = \alpha_F^{-2} . \tag{66}$$

Then $D_{-\infty}^F$ and D_{∞}^F are related to σ_{00} and σ_{11} in the following way:

$$D_{-\infty}^F = -\frac{\log 2}{\log \sigma_{00}} , \quad D_{\infty}^F = -\frac{\log 2}{\log \sigma_{11}} . \tag{67}$$

Table 2.

2^m	a	σ_{00}	σ_{11}	$\sigma_{01}\sigma_{10}$	$-\frac{\log 2}{\log \sigma_{11}}$	$-\frac{\log 2}{\log \sigma_{00}}$
8	2.000	0.2091	0.0857	0.0210	0.282	0.443
16	2.00	0.2613	0.1062	0.0315	0.309	0.517
32	1.999	0.2852	0.1160	0.0404	0.322	0.553
64	1.999	0.3029	0.1234	0.0458	0.331	0.580
∞	2.000...	0.399...	0.1596	0.0722	0.377...	0.755...

With high enough acuracy, these equalities are valid also for the limit cycles, compare 2nd and 4th columns of Table 1 and the 6th and 7th columns of Table 2.

Thus, the transfer matrix method allows one unambiguously to find the origin of the limit cycles:
— they are self-similar, if the scale of the fractal cover is successively doubled ($\alpha = 2$);
— two scales take part in their construction (σ_{00} and σ_{11}), converging towards α_F^{-1} and α_F^{-2}, respectively;
— no transfer matrix element is zero.

The only dynamics obeying all these conditions is that of period doublings generated by Poincare maps with a quadratic maximum. If some other fractal under consideration exhibits the same properties of the transfer matrix elements then one can be sure that the underlying dynamics is that of period doubling. The transfer matrix method was successfully applied to the data processing in the Benar experiment [44].

3.4 Analysis of events in hadron collisions

Armed by such a promising technique, let us use the matrix transfer method to analyse the events that occur in hadron–hadron collisions. Let us assume that the coordinates of the observed particles in the momentum space form a finite set which is an approximation of some unknown fractal [46], the dynamics of which we want to reveal. This approach to hadron physics has recently become a powerful instrument for the investigation of multiple formation of particles [12].

For simplicity, let us consider a one-dimensional section of the momentum space, which is the rapidity axis, and denote the rapidities of the observed particles by y_i. There is a clear analogy with the one-dimensional Poincare section of some multidimensional phase trajectory such that the rapidities of the observed particles correspond to the point of intersection of this trajectory and the Poincare section.

It should be stressed that our interpretation of the relationship between the multiplicity of particle collisions and the Ising model differs radically from the usual interpretation found in the literature [47, 48]. Usually a particle on the rapidity axis is assigned a spin variable whose value is 1 on an Ising chain (spin 0 corresponds to the absence of a particle) and the transfer matrix reflects the interaction of such spins. Naturally, this approach cannot be used to extend the treatment to more complex Ising chains when at each site there may be more than two spin states and/or the interaction involves more than just the nearest sites in a chain.

However, in our model the particles are not assigned spin variables and these variables appear only in the course of transition between different partitions formed from the same set of particles on the rapidity axis. This set is regarded as an approximation of some infinite fractal set. In our approach the 'spin–spin interaction' is a 'topological' characteristic of a fractal and it is in no way related to correlations in the positions of real particles on the rapidity axis. Our model can be generalised to more complex Ising chains, which seems to be a very promising field for investigation, but this is outside the scope of the present review.

For comparison, let us consider two experimental events: the well-known anomalous event reported by the NA22 collaboration [49], who investigated the π^+p interaction with the centre-of-mass energy $\sqrt{s} = 22$ GeV, and

Table 3.

n_{tot}	D_∞	D_0	$D_{-\infty}$	a	σ_{00}	σ_{11}	$\sigma_{01}\sigma_{10}$	$-\frac{\log 2}{\log \sigma_{11}}$	$-\frac{\log 2}{\log \sigma_{00}}$
26	0.337	0.811	1.241	2.000	0.550	0.125	0.238	0.334	1.16
24	0.326	0.666	1.181	1.999	0.558	0.117	0.120	0.324	1.19
22	0.315	0.737	1.163	1.999	0.579	0.108	0.166	0.312	1.27
20	0.302	0.568	0.975	2.000	0.470	0.098	0.089	0.299	0.918
18	0.288	0.657	1.066	2.000	0.608	0.088	0.101	0.286	1.39
16	0.273	0.492	0.881	2.000	0.458	0.076	0.049	0.270	0.888
119	0.487	0.782	1.37	1.999	0.609	0.241	0.140	0.488	1.40

the event recorded by the JACEE collaboration when a cosmic-ray silicon nucleus interacted with a photographic emulsion at an energy of about 4 TeV per nucleon (Si–AgBr interaction) [50]. In the case of the NA22 event, the dependence $q(\tau)$ was found by the same-weight method [see expression (39)], since the rapidities of all 26 particles are known accurately ($\Delta p/p < 2\%$). The complete integral [0, 1] by a smooth transformation, $x_i = (\tanh y_i \bar{1})/2$, and all the particles — beginning from the first — were combined into pairs with the nearest neighbour on the x axis. The diameter δ_i was calculated from formula (37).

In the case of the JACEE event, we determined the dependence $\tau(q)$, expressed in terms of the moments G_q [defined by expression (40)], since in the case of this event only the histogram $dN/d\eta$ was known with the bin size 0.1 on the pseudorapidity scale. We analysed only the part of the histogram above the smooth background [51, 52], representing 119 particles out of the total number of charged particles $n_{\text{ch}} = 1010 \pm 30$.

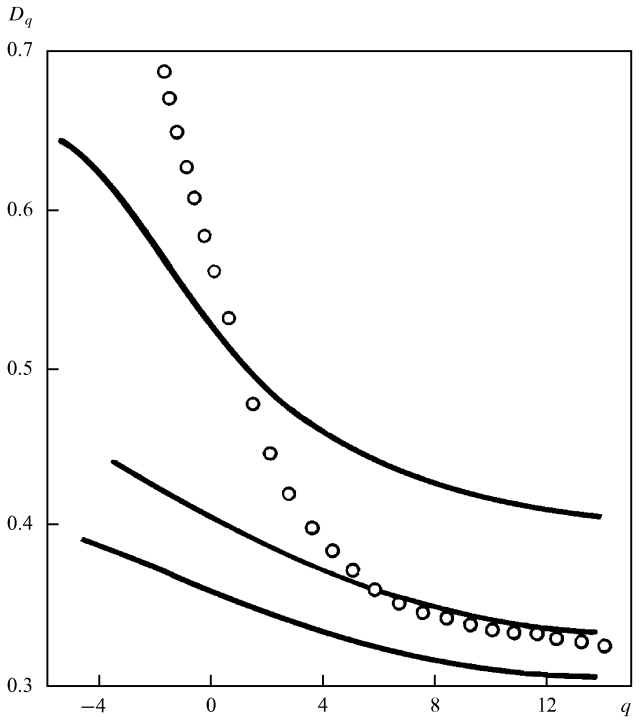

Figure 2. Dependences of the Renyi dimensions D_q on q for the Feigenbaum attractor (curve *1*), for the limits 16 an d18 cycles (curves *2* and *3*, respectively) and for the anomalous event reported by the NA22 collaboration [49] circles (labelled *4*), analysed on the basis of just 20 central particles.

Earlier, in determination of the Renyi dimensions and of the transfer matrix elements, we selected for each event its own value $\tau(0)$ and three arbitrarily selected other values of $\tau(q)$ (see also the comment in Section 3.3), which we then substituted in expression (63). The resultant system of four nonlinear equations was solved numerically by the multidimensional Newton method.

The results are presented in Table 3, where the last row ($n_{\text{tot}} = 119$) corresponds to the JACEE event and the other rows represent the NA22 event. The first column gives the number of particles included in our analysis: we dropped successively two outermost particles (one from the front hemisphere and the other from the rear hemisphere) and we thus selected the central interaction zone.

The transfer matrix method revealed, for both events, the doubling dynamics ($a = 2$), the fact that all the matrix elements have nonzero values, and ensured a reasonable agreement between the theoretical (in the region of the 8, 16, 32 cycles) and experimental values of the matrix element σ_{11}, which is responsible for the parts of the fractal with the highest density of the elements. Moreover, the D_q dependence for the NA22 event with 20 central particles was found to be almost identical with the D_q dependence for the limit 16 cycle when $q \geqslant 6$ (Fig. 2). It was found that this near-identity is not accidental and in the next section I shall consider briefly the bifurcation model which accounts for this.

3.5 Bifurcation model

A bifurcation model was proposed by me in 1992 [33] to account for the intermittency in the rapidity distributions of charged particles formed at high energies [6, 11, 12]. The main assumptions made in the bifurcation model are as follows:

(1) there is a nonlinear equation which controls the dynamics of quarks and gluons, and the solutions of this equation depend on just one parameter which is the energy $\sqrt{\hat{s}}$ of a collision in a single event;

(2) the number of partitions of the phase trajectory corresponding to a given solution determines the number of intermediate particles (the number of clans), which may decay into the observed particles;

(3) the number k of the particles in each decay may vary, but the average over all the decays and events remains constant for different energies:

(4) on the phase trajectory there is a one-dimensional Poincare section which has a single quadratic maximum if the direction of this section in the phase space is selected along the rapidity axis.

In other words, after some transformations, we can write down the Poincare map in the form of a logistic map,

described by expression (45), where the governing parameter λ depends on the collision energy as follows [33]:

$$\lambda \approx \lambda_\infty - \frac{1}{3\sqrt{\hat{s}}}, \tag{68}$$

where $\sqrt{\hat{s}}$ is the collision energy in gigaelectron-volts. We recall that, for each value of the governing parameter $\lambda \in [3, \lambda_\infty]$ there is one and only one stable limit 2^m cycle ($m = 1, 2, 3, \ldots$) in a unit interval [0, 1]. The position of each element in a cycle can be calculated with any desired precision. The complete interval on the rapidity axis $[-y_{\max}, y_{\max}]$ is mapped onto [0, 1] by a smooth transformation, such as $(\tanh y + 1)/2$, which does not alter the topological characteristics of the initial fractal set (formed by clans).

Consequently, for any energy $\sqrt{\hat{s}}$ of a collision in a given event we can use formula (68) to find the corresponding value of λ and, consequently, the corresponding 2^m cycle. This is the key feature of the bifurcation model: the observed distributions of particles in the momentum phase space (in particular, the rapidity distributions) are simply 'pictures' of the distributions of the elements of the limit 2^m cycles in a unit interval.

The decay of clans into secondary particles reduces the density of the initial fractal set and this increases the observed Renyi dimensions D_q with $q < 0$, compared with the true dimensions D_q. This is the reason why, in the bifurcation model framework, there is some discrepancy between the values of the matrix element σ_{00} responsible for the parts of the fractal with the minimal particle density.

This is supported also by the values of $D_{-\infty}$, D_0, and D_∞ for the JACEE event, which are identical with the corresponding average values for the events involving collisions of heavy ions [53]. One should point out also that equality (67) for the experimental events is satisfied with high precision (compare second and fourth, and also ninth and tenth columns in Table 3), particularly in the case of D_∞ and σ_{11}, undistorted by the clan decays. Consequently, the transfer matrix elements for the observed experimental events can be obtained directly from D_∞, D_0, and $D_{-\infty}$ even without solving Eqn (63).

For D_1 with $q > 0$ and particularly with $q \gg 1$, responsible for the densest parts of the fractal, we can expect very small deviations from the true values of D_q. In fact, if the clans decay isotropically and independently of one another, the probability that several π mesons are within a certain rapidity interval is proportional to the size of the interval. Consequently, the smaller the interval, i.e. the higher the density of particles in this interval, the lower is the probability of random 'imitation' of the true fractal dimension by the secondary π mesons.

The question is: are there any other characteristics of multiparticle production, apart from D_q for $q \gg 1$, that are predicted by the bifurcation model and which permit direct comparison with experiments? The answer is 'yes', and we shall consider this answer in the next section.

3.6 Feigenbaum universality and period-doubling dynamics in hadron physics

The next characteristic of the limit 2^m cycle which can be used in comparison with experiments is the dependence of the maximum number of elements $n_{\max}$ within a fixed interval $\delta\xi$ on the value of $\delta\xi$.

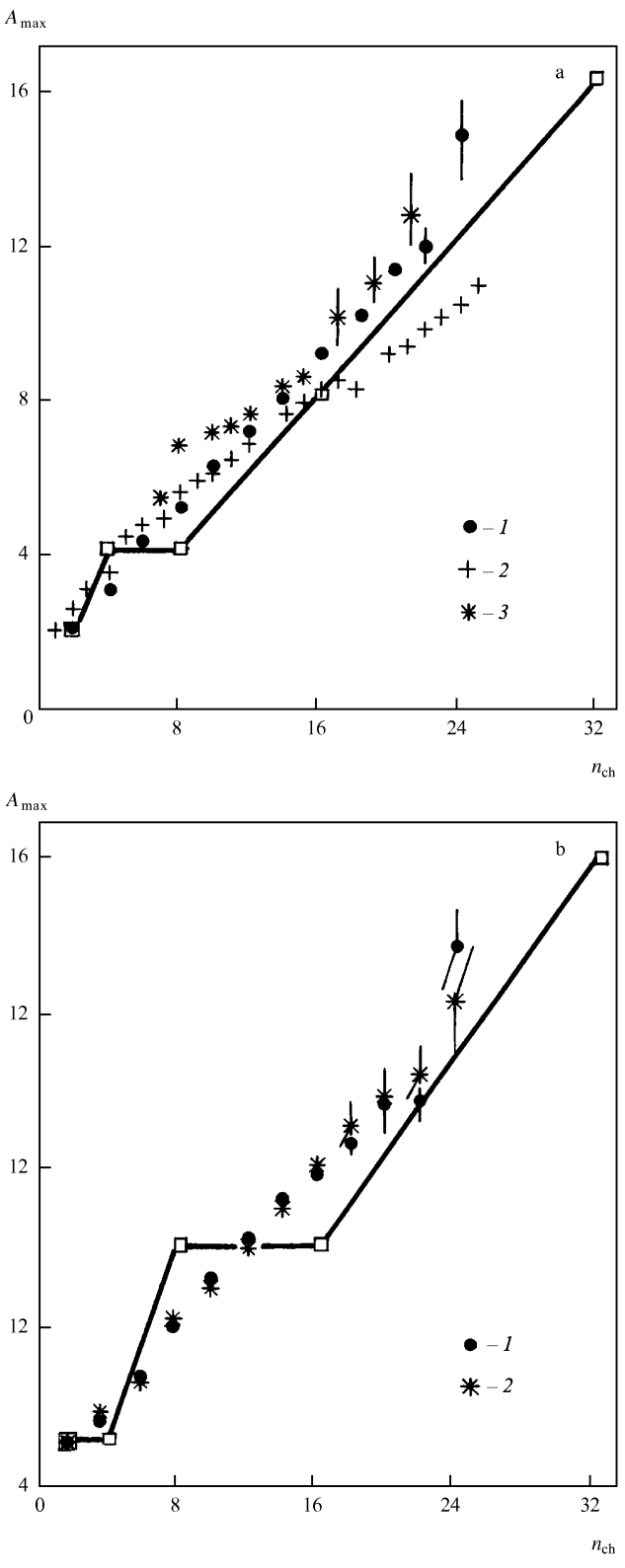

Figure 3. Dependences of A_max on n_{ch}, described by expression (69), plotted for $\Delta\eta = 0.5$ (a) and $\Delta\eta = 0.1$ (b). Experimental points: (a) symbols labelled *1* represent π^+p collisions with $\sqrt{s} = 22$ GeV [49], symbols labelled *2* represent $\bar{\text{p}}$p collisions with $\sqrt{s} = 540$ GeV [54], symbols labelled *3*, represent the p–AGBr interaction for $p_{\text{lab}} = 400$ GeV/c [55]; (b) symbols labelled *1* represent the π^+p collisions with $\sqrt{s} = 22$ GeV [49], symbols labelled *2* represent pp collisions with $\sqrt{s} = 22$ GeV. The theoretical predictions are given by the open squares which, for the same of convenience, are joined by rectilinear segments.

The theoretical dependence of $n_{\max}(\delta\xi)/\delta\xi$ found experimentally corresponds to the maximum particle density $A_{\max}$, defined as follows:

$$A_{\max} \equiv \left\langle \frac{\Delta n_{\max}}{\Delta\eta} \right\rangle , \tag{69}$$

where $\Delta\eta$ is a fixed interval of the pseudorapidity; $\Delta n_{\max}$ is the maximum number of particles in the interval $\Delta\eta$, which is found by scanning the complete pseudorapidity interval η with the interval $\Delta\eta$ for each event, following by averaging over all the events ($\langle \ldots \rangle$). Fig. 3 gives the values of $A_{\max}$ for the π^+p, pp [49], $\bar{\text{p}}$p [54], and p-AgBr [55] interactions at various energies for two fixed pseudorapidity intervals $\Delta\eta$: $\Delta\eta = 0.5$ and 0.1.

It follows from the bifurcation model that a number of clans created in particle collisions can only be 2^m, where $m = 1, 2, 3, \ldots$. All the intermediate values for the set result from the decay of clans into secondary hadrons. Consequently, the bifurcation model predicts the value of $n_{\max}(\delta\xi)$ only for the clans, i.e. for the 2^m sets which are regarded as the corresponding sizes of the cycles. Our calculations can be compared with the experimental results if we know the correspondence between $\Delta\eta$ and $\delta\xi \in [0, 1]$. We shall do this by finding the maximum number of bins

$$M_{\max}^{\exp} = \frac{2y_{\max}}{\Delta\eta} \tag{70}$$

for each experiment and by equating it to the theoretical value:

$$M_{\max}^{\exp} = M_{\max}^{\text{theor}} = M_{\max} . \tag{71}$$

We then have the following correspondence:

$$\Delta\eta \Leftrightarrow \delta\xi = \frac{1}{M_{\max}} . \tag{72}$$

it should be noted that the value of $y_{\max}$ for the set 2^m is not taken from experiments but from the relationship

$$y_{\max} = \log \frac{(\sqrt{s})_{m+1} - 2m_N}{m_\pi} , \tag{73}$$

where n_{N} (m_π) is the mass of a nucleon (π meson); $(\sqrt{s})_{m+1}$ is the threshold energy for the appearance of the next 2^{m+1} cycle [see expression (68)]. For $m = 1, 2, \ldots, 6$, the corresponding energies $(\sqrt{s})_m$ are (in gigaelectron-volts):

m	1	2	3	4	5	6
$(\sqrt{s})_m$	1.00	4.67	21.8	102	475	2218

(74)

Therefore, for each value of $\sqrt{s}$ and a fixed value of $\Delta\eta$ we can find the corresponding 2^m cycle from the above tabulation and we can identify the corresponding bin size $\delta\xi \in [0, 1]$ from expression (72). The quantity $\delta\xi$ is then used to scan the whole unit interval in order to find $n_{\max}(\delta\xi)$ and the result is the quantity $n_{\max}(\delta\xi)/\Delta\eta$ (see Fig. 3). The agreement between the theory and experiment is quite satisfactory. In fact, the bifurcation model explains the experimentally observed [49, 55] unity slope of the dependence $A_{\max}(n_{\text{ch}})$ at high values of n_{ch}:

$$A_{\max} = an_{\text{ch}} + b , \quad a_{\text{theor}} = 1 , \tag{75}$$

which is a consequence of the self-similar structure of the 2^m cycles. In other words, any finite part of the unit interval containing a sufficient number of the elements of the 2^m cycle can reproduce the structure of the other 2^n cycles, where $n > m$. If the resolution is fixed, the only difference is the increasing (doubling) number of the cycle elements within the interval $\delta\xi$. As a result, the value of $n_{\max}$ doubles at each $m \to m + 1$ transition. The larger the value of $\delta\xi$ (or $\Delta\eta$ in the experiments), the earlier (i.e. for smaller sets) can we observe such a self-similarity and, consequently, a linear dependence $A_{\max}(n_{\text{ch}})$. In fact, it is evident from Fig. 3 that formula (75) is obeyed for $n_{\text{ch}} \geqslant 8$ and $\Delta\eta = 0.5$, whereas for $\Delta\eta = 0.1$ this formula is valid only for $n_{\text{ch}} \geqslant 16$. It should be noted that in the trivial case of a uniform distribution of particles in accordance with their rapidity, the linear rise of $\Delta\max(n_{\text{ch}})$ can be observed beginning directly from $n_{\text{ch}} = 2$ and extending to infinity.

I think it would be more interesting to determine the inverse dependence $n/\Delta\eta_{\min}(n)$ for a fixed collision energy. Let us begin by selecting events with the same number n_{tot} of charged particles. Then, for each fixed value of $n = 2, 3, 4, \ldots < n_{\text{tot}}$, we can find — for each event — that the minimum pseudorapidity or rapidity interval $\Delta\eta_{\min}(n)$ which contains a given number of charged particles; we can then average the result over all the events. It is desirable to make this analysis for sets of events for which the total number n_{tot} differs by a factor of 2: for example, $n_{\text{tot}} = 2\langle n_{\text{ch}} \rangle$, $\langle n_{\text{ch}} \rangle$, and $\frac{1}{2}\langle n_{\text{ch}} \rangle$.

A similar $n/\delta\xi_{\min}(n)$ dependence can be calculated analytically for the limit 2^m cycles on the basis of formula (13) with $\tau = 1$:

$$\frac{n}{\delta\xi_{\min}(n)} \propto \delta\xi_{\min}^{-\nu} , \quad \nu = 1 - \frac{1}{q(1) - 1} , \tag{76}$$

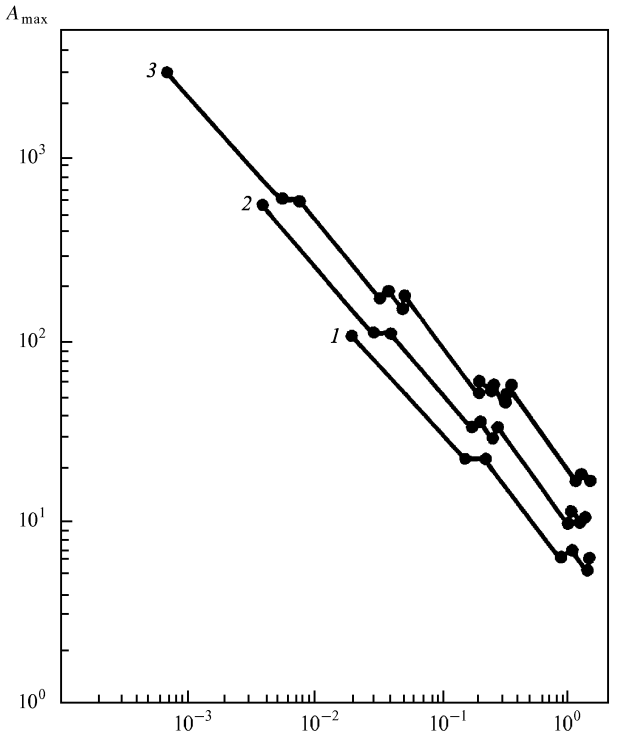

Figure 4. Dependences of the quantity $n/\Delta\eta_{\min}(n)$ (represented by $A_{\max}$) on $\Delta\eta_{\min}$, plotted for the limit 16, 32 and 64 cycles (curves *1*, *2*, and *3*, respectively).

which gives — for example — the values $\nu = 0.628$ and $\nu = 0.605$ for the 16 and 32 cycles, respectively. In the case of the Feigenbaum attractor, we have

$$q(1) = \frac{\log(\alpha_F^2 + \alpha_F)}{\log 2} = 3.132158\ldots , \tag{77}$$

which gives $\nu = 0.53099\ldots$. We also found numerically the value of $\delta\xi_{\min}(n)$ for $n = 2, 3, 4, \ldots$ for the limit 16, 32, and 64 cycles. This made it possible to plot in Fig. 4 the quantity $n/\Delta\eta_{\min}(n)$ (represented by $A_{\max}$) as a function of $\Delta\eta_{\min}$. The quantity $\Delta\eta_{\min}$ is defined as usual [see expressions (70)–(72)]:

$$\Delta\eta_{\min} = 2y_{\max}\delta\xi_{\min} . \tag{78}$$

The extreme point on the left on each curve in Fig. 4 corresponds to $n = 2$. All these curves fit well a straight line with the slope -0.65 ± 0.03 [see the set of expressions (76)].

However, in real experiments [56] the measured quantity, closely related to the quantity under consideration here, was the 'entropy' S considered as a function of the size of the symmetric interval $|y| \leqslant y_c$ of the rapidity. The entropy S is defined by

$$S = (n_{ch} + 1)\ln(n_{ch} + 1) - n_{ch}\ln n_{ch} , \tag{79}$$

where n_{ch} is the number of charged particles in the interval $|y| \leqslant y_c$. If we regard $S/y_{\max}$ as a function of the scaling variable $\ln(y_c/y\,ax)$, where — as usual — we have $y_{\max} = \ln(\sqrt{s} - 2m_N)/m_\pi$, we find that the bulk of the curve is a straight lie with a slope $(\sim 0.090 \pm 0.002)$ which is insensitive to $\sqrt{s}$ (Fig. 5) [56]. If the dependence $n_{ch}(y_{ch})$ is written in the form

$$n_{ch} = \left(\frac{\sqrt{s}}{m_{\pi\perp}}\right)^{\beta(y_c/y_{\max})} , \tag{80}$$

like the approximation [57] for the data of the set of $\bar{p}p$ collisions in the energy range $\sqrt{s} = 5 - 900$ GeV,

$$\langle n_{tot}\rangle = \left(\frac{\sqrt{s}}{m_{\pi\perp}}\right)^{\beta} , \tag{81}$$

where $\beta \equiv \beta(1) = 0.449 \pm 0.018$, $m_{\pi\perp} = 0.231$ GeV, we can readily see that $S/y_\beta(y_c/y_{\max})$ for n_{ch}. The theoretical value of β is given by the formula [58]

$$\beta \equiv \beta(1) = \frac{\log 2}{\log \delta_F} = 0.449806\ldots , \tag{82}$$

where δ_F is the second Feigenbaum constant [see expression (46)].

Next, it follows from expression (81) that

$$\ln\langle n_{tot}\rangle \approx \beta y_{\max} , \tag{83}$$

and we than have

$$\frac{S}{y_{\max}}\beta\frac{\ln n_{ch}}{\ln n_{tot}} . \tag{84}$$

What does the bifurcation model say about the right-hand side of the above approximation equality? Let us assume the correspondence $\delta\xi_{\min} \Leftrightarrow y_c/y\,ax$. Then the number of elements in a specific 2^m cycle, which lies within an interval of length $\delta\xi_{\min}$, agrees with the experimental value of n_{ch} in the interval $|y| \leqslant y_c$. Applying again expression (13) with $\tau = 1$, we obtain

$$\beta\frac{\ln n_{ch}}{\ln n_{tot}} = \frac{\beta}{(q-1)\ln n_{tot}}\ln\delta\xi_{\min} + \beta , \tag{85}$$

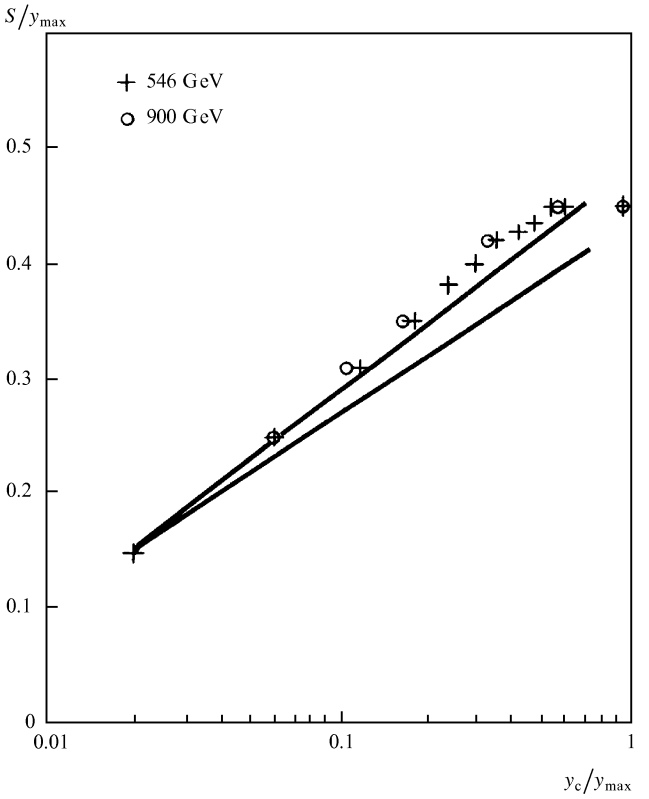

Figure 5. Dependences of the normalised entropy $S/y_{\max}$ on the scaling variable $y_c/y_{\max}$. The experimental pints correspond to the $\bar{p}p$ collisions with $\sqrt{s} = 546$ GeV [59] and 900 GeV [60]. The theoretical lines correspond to the limit 4 and 8 cycles (*1* and *2*, respectively).

i.e. the theory does indeed predict — on a logarithmic scale — a straight line with the slope

$$k = \frac{\beta}{(q-1)\ln n_{tot}} .$$

The slopes for the 4, 8, and 16 cycles are $k = 0.083$, 0.072, and 0.060 respectively, which is in reasonable agreement with the experimental slope 0.090 ± 0.002 (Fig. 5). We must also take into account that, first, the theory reflects the positions of the clans on the rapidity axis and that their decay into secondary particles changes somewhat the slope of this straight line; second, the theory predicts the slope on the assumption that y_c is the minimum distance along the rapidity axis needed to 'cover' a given number of particles, whereas the experimental value of y_c is known to be greater than or equal to the theoretical value.

Consequently, from the point of view of the bifurcation model, it would be preferable to determine the quantity $B \equiv \ln(n_{ch}/n_{tot})$ as a function of the scaling variable $y_c/y_{\max}$. Here, y_c denotes the minimum interval $|y| < y_c$ which contains the given number n_{ch} of charged particles. For the corresponding limit cycles [see expression (13)], the quantity B is

$$B = \frac{1}{q(1)-1}\ln\delta\xi_{\min}(n) . \tag{86}$$

The values of $1/[q(1) - 1]$ for the limit 8, 16, and 32 cycles are 0.335, 0.372, and 0.395, respectively.

4. Conclusions

This review provides a brief account of the evolution, for over a century, of the mathematical apparatus needed to investigate fractals, beginning from the Cantor concept of the cardinality of an infinite set to the generalised Renyi dimensions. We became acquainted with the topological Lebesque dimension and with dimension proposed by Brauer, and by Urison and Menger. We also considered the concept of a measure and of the Hausdorff dimension, which depend on the metric of the topological space. At the end of Section 2, we also encountered the initial information on a new method for investigating fractals, which is stochastical analysis.

In Section 3, we applied the mathematical apparatus introduced earlier to one of the best known fractals, discovered recently literally in all branches of physics, which is the Feigenbaum attractor. We became acquainted with the transfer matrix method, relating the processes of successive increasingly accurate covering of a given fractal to the theory of the transfer matrices of the corresponding Ising model. This method provides means for extracting information on the dynamics of a process generating a given fractal and has earlier been applied successfully to turbulence in the physics of liquids. We applied this method to two events of multiple formation of particles in hadron–hadron collisions and showed that the dynamics responsible for a given particle distribution on the rapidity axis is very probably the period-doubling dynamics which, for infinite collision energies, leads to the Feigenbaum attractor.

This result may have far-reaching consequences. First, the existence of the Feigenbaum universality narrows down significantly the class of equations which can pretend to the role of control of the dynamics of the hadron-creation processes, since in this case they should have solutions with a quadratic singularity on the appropriate Poincare map.

Second, generalisation of the Feigenbaum universality to relativistic processes makes it possible to use many results of the unimodel mapping theory in hadron physics. In particular, on the basis of this hypotheses, it is possible to calculate in a parameter-free manner, the exponents representing the growth with energy of the average multiplicity of particles in different rapidity intervals [33], the multiplicity dependence of the maximum particle density per unit rapidity [33, 51], and the ratio of the lengths and heights of steps considered as a function of the average transverse momentum on the multiplicity when the collision energy is fixed [35].

The next step should be a study, by the transfer matrix method, of 'ordinary' events in hadron–hadron and nucleus–nucleus collisions, and also in the e^+e^- annihilation process, since the period-doubling dynamics (if it does exist) should describe all the events.

Acknowledgements. I am grateful to I V Andreev, I M Dremin, and A K Likhoded for valuable comments, and to M T Nazirov and V V Levchenko for helpful discussions. This work was supported by the Russian Foundation for Basic Research (Grant No. 94-02-03314).

References

1. Mandelbrot B B *The Fractal Geometry of Nature* (New York: W H Freeman, 1982)
2. *Fractals in the Natural and Applied Sciences* (Proceedings of the Second IFIP Working Conference, London, 1993, Ed. M M Novak) (Amsterdam: North-Holland, 1994)
3. Konishi K, Ukawa A, Veneziano G *Nucl. Phys. B* **157** 45 (1979)
4. Giovannini A *Proceedings of Tenth International symposium on Multiparticle Dynamics, Goa, India, 1979* p. 364
5. Carruthers P, Mihn Duong Van, Los Alamos Report LA-UR-83-2419 (1983)
6. Bialas A, Peschanski R *Nucl. Phys. B* **273** 703 (1986)
7. Dremin I M *Pis'ma Zh. Eksp. Teor. Fiz.* **45** 505 (1987) [*JETP Lett.* **45** 643 (1987)]
8. Zel'dovich Ya B, Sokolov D D *Usp. Fiz. Nauk* **146** 493 (1985) [*Sov. Phys. Usp.* **28** 608 (1985)]
9. Paladin G, Vulpiani A *Phys. Rep.* **156** 147 (1987)
10. Zel'dovich Ya B, Molchanov S A, Ruzmaikin A A, Sokolov D D *Usp. Fiz. Nauk* **152** 3 (1987) [*Sov. Phys. Usp.* **20** 353 (1987)]
11. Dremin I M *Usp. Fiz. Nauk* **160** (8) 105 (1990) [*Sov. Phys. Usp.* **33** 647 (1990)]
12. De Wolf E A, Dremin I M, Kittel W *Usp. Fiz. Nauk* **163** 3 (1993)
13. Schertzer D, Lovejoy S *Physica A* **185** 187 (1992)
14. Dokshitzer Yu L, Dremin I M *Nucl. Phys. B* **402** 139 (1993)
15. Dremin I M, Nazirov M T *Yad. Fiz.* **55** 197 (1992)
16. Hwa R C *Phys. Rev. D* **47** 2773 (1993)
17. Cantor G *J. Reine Angew. Math.* **77** 258 (1874)
18. Klein F *Elementary Mathematics from an Advanced Standpoint*, Vol. 1 *Arithmetic, Algebra, Analysis* (New York: Macmillan, 1932; reprint — New York: Dover, 1945)
19. Peano G *Math. Ann.* **36** 157 (1890)
20. Poincare H *Rev. Methaphys. Morale* 486 (1912)
21. Brouwer L E *J. Math.* **142** 146 (1913)
22. Aleksandrov P S *Kombinatornaya Topologiya* (Combinatoric Topology) (Moscow: OGIZ Goztekhizdat, 1947)
23. Gurevich V, Volmen G *Theory of Dimensions* (translated into Russian) (Moscow: Inostr. Literatura, 1948)
24. Lebesgue H *Math. Ann.* **70** 166 (1911)
25. Mazurkevich A *Fund. Math.* **10** 311 (1927)
26. Hausdorff F *Math. Ann.* **79** 157 (1919)
27. Pontryagin L, Shnirelman L *Ann. Math.* **33** 156 (1932)
28. Shuster H G *Deterministic Chaos: an Introduction*, 2nd edition (Cambridge, England: VCH Publishers-UK, 1987)
29. Halsey T C, Jensen M H, Kadanoff L P, et al. *Phys. Rev. A* **33** 1141 (1986)
30. Brax P, Peschanski R *Phys. Lett. B* **253** 255 (1991)
31. Ratti S P, Salvadori G, Gianini G, et al. *Z. Phys. C* **61** 229 (1994)
32. Chiu C B, Hwa R C *Phys. Rev. D* **43** 100 (1991)
33. Batunin A V *Yad. Fiz.* **55** 2525 (1992) [*Sov. J. Nucl. Phys.* **55** 1407 (1992)]
34. Batunin A V *Yad. Fiz.* **57** 1078 (1994) [*Phys. At. Nucl.* **57** 1017 (1994)]
35. Batunin A V *Phys. Lett. B* **318** 391 (1993)
36. Batunin A V, Sergeev S M *Phys. Lett. B* **327** 293 (1994)
37. Sharkovskii A N, et al. *Dinamika Odnomernykh Otobrazhenii* (Dynamics of One-Dimensional Mapping) (Kiev: Naukova Dumka, 1989)
38. Vul E B, Sinai Y G, Khanin K M *Usp. Mat. Nauk* **30** (3) 3 (1984)
39. Feigenbaum M J *Los Alamos Science* **1** (1) 4 (1980)
40. Feigenbaum M J *J. Stat. Phys.* **19** 25 (1978); **21** 669 (1979)
41. Feigenbaum M J *Commun. Math. Phys.* **77** 65 (1980)
42. Poincare H *Am. J. Math.* **7** 213 (1885)
43. Cvitanovic P *Universality in Chaos* (Bristol: Adam Hilger, 1984)
44. Feigenbaum M J, Jensen M H, Procaccia I *Phys. Rev. Lett.* **57** 1503 (1986)
45. Baxter R J *Exactly Solved Models in Statistical Mechanics* (New York: Academic Press, 1982)

46. Dremin I M, in *Multiparticle Dynamics: Festschrift for Leon Van Hove* (Eds A Giovannini, W Kittel) (Singapore: World Scientific, 1989) p. 455
47. Chau L L, Huang D W *Phys. Lett. B* **283** 1 (1992)
48. Seixas J *Mod. Phys. Lett. A* **6** 1237 (1991)
49. Adamus M, Ajinenko I V, Amato S F, et al. (NA22 Collab.) *Phys. Lett. B* **185** 200 (1987)
50. Burnett T H, Dake S, Fuki M, et al. (JACEE Collab.) *Phys. Rev. Lett.* **50** 2062 (1983)
51. Batunin A V *Proceedings of Twelth International Conference on Noise and Physical Systems and 1/f Fluctuations, St Louis, MO, 1993* (Eds P H Handel, A L Chung) p. 569
52. Takagi F *Phys. Rev. Lett.* **53** 427 (1984)
53. Shivpuri R K, Verma V K *Phys. Rev. D* **47** 123 (1993)
54. Geich-Gimbel C (UA5/2) Preprint HE-85-36 (Bonn: University, 1985)
55. Ghosh D, Sen S, Roy J *Phys. Rev. D* **47** 1235 (1993)
56. Carruthers P A, Plumer M, Raha S, Weiner R M *Phys. Lett. B* **212** 369 (1988)
57. Batunin A V, Yuschenko O P *Mod. Phys. Lett. A* **5** 2377 (1990)
58. Batunin A V, Preprint IHEP 87-91 (Protvino, Moscow Province: Institute of High Energy Physics, 1991)
59. Aluer G J, et al. (UA5) *Phys. Lett. B* **121** 209 (1983); Alner G J, Alpgard K, Anderer P, et al. *Phys. Lett. B* **160** 193 (1985)
60. Alner G J, Ansorge R, Asman B, et al. (UA5) *Phys. Lett. B* **167** 476 (1986)